Fractional and Integer Charge Transfer at Semiconductor/Organic Interfaces: The Role of Hybridization and Metallicity

Simon Erker[a], Oliver T. Hofmann[a]*

[a] *Institute of Solid State Physics, Graz University of Technology, NAWI Graz, Petersgasse 16, 8010 Graz Austria*

**Corresponding Author: o.hofmann@tugraz.at*

ABSTRACT

Inorganic/organic interfaces show two phenomenologically different types of charge transfer: On inert substrates, a coexistence of charged and neutral molecules is found, while on metals, which have more available charge carriers and a larger propensity to hybridize, the organic component is homogeneously, fractionally charged. In this contribution, we use hybrid density functional theory to study the adsorption of the strong electron acceptor F4TCNQ on ZnO(10-10) as function of the substrate's doping concentration. This system undergoes a joint charge donation/backdonation reaction. Since the former is driven by hybridization, but the latter is not, this allows us to discuss the impact of hybridization and charge carrier availability separately. We find that while the hybridization determines the mechanism, the charge-carrier concentration (i.e., "metallicity") crucially impacts the amount of transferred charge. This leads to the situation that at low doping concentrations, most of the molecules basically neutral and the transferred charge is localized on individual molecules.

TOC GRAPHIC

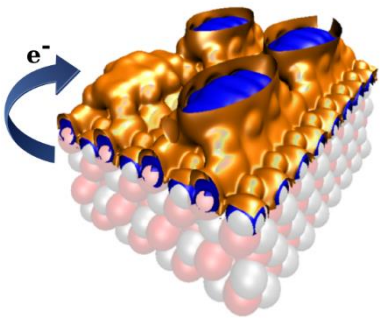

Hybrid interfaces between inorganic semiconducting materials and organic molecules represent particularly interesting systems to study fundamental quantum-mechanical effects, since the flexibility of organic chemistry and the adjustability of the inorganic substrate's free charge-carrier concentration allows systematically tuning the strength of the interaction between the two components. Also from a practical viewpoint, the properties of organic and inorganic materials complement each other, which already led to many practical applications, such as light-emitting diodes for displays, lighting applications[1,2] or organic photovoltaic cells.[3,4] Other applications are still in their infancy, such as organic thermoelectric materials,[5] molecular switches,[6,7] or spintronic[8] devices. For their final success, an in-depth atomistic understanding of the quantum processes at the relevant interfaces is critical. Of particular interest in this context is the nature and mechanism of charge-transfer across the interface, since this critically affects the device performance.

Experimental investigations of inorganic/organic interfaces often find that the average charge-transfer amounts to less than a full electron per molecule. This allows for two different interpretations: Either, the charge is transferred in integer units and is localizes on individual molecules, which leads to a co-existence of integer charged and uncharged molecules. This is known as the integer charge transfer (ICT) model.[9–11] Alternatively, the charge delocalizes within the organic layer, leading to a homogeneous

distribution of fractionally charged molecules. This is called the fractional charge transfer (FCT) model.[9,12] Experimentally, localized charge is mainly observed for adsorption on inert substrates, such as semiconductors or passivated metals[10,11,13,14] . Conversely, delocalized charges are found for adsorption on weakly reactive metal surfaces.[15–19]. Thus, there seem to be two properties of the *substrate* that potentially influence the charge-transfer mechanism: the propensity to hybridize with the adsorbate, and the availability of free charge-carriers. Although these properties are often correlated (i.e., metals have a larger charge-carrier concentration and tend to be more reactive than semiconductors), they are not necessarily causally related. The open question at the heart of this contribution is to what extend these two different aspects impact the charge-localization at the interface.

Ideal systems to address this issue are monolayers of small organic molecules on weakly reactive substrates, which are in between the prototypical cases of physisorption (i.e., inert systems) and chemisorption (i.e., the formation of covalent bonds between substrate and adsorbate). In this study, we use theoretical modeling based on hybrid density functional theory to exemplarily investigate the adsorption of tetrafluorotetracyanoquinodimethane (F4TCNQ) on the wide-bandgap semiconductor ZnO. We focus on the question how the localization of charge is affected when the nature of the substrate is gradually changed from insulating to metallic by tuning its free charge-carrier concentration.

Zinc oxide is a prototypical semiconducting oxide that has attracted significant attention for use in organic electronic devices due to its optical transparency and wide band gap (E_g = 3.4 eV).[20,21] Natively grown, ZnO has a free carrier concentration below 10^{16} cm^{-3},[22] while highly doped ZnO, on the other hand, can reach carrier concentrations up to 10^{21} cm^{-3}. [23–25] The chosen adsorbate, F4TCNQ (see inset of Figure 1a), is a prototypical organic acceptor that is used both in practical applications[26,27] and in many surface science studies.[10,16,28–32] It is susceptible to both charge-transfer mechanisms, depending on the nature of the substrate.[10,16]

Furthermore, F4TCNQ can undergo charge-transfer via two separate "channels": One the one hand, the peripheral cyano groups can form dative covalent bonds, donating electrons to the substrate ("charge donation"). On the other hand, the energetically low-lying lowest unoccupied molecular orbital (LUMO) readily accepts electrons from the Fermi-level ("charge backdonation")[16] of materials with a sufficiently low work function.[9,33]. Since the latter process occurs because of a difference between the electron affinity of the adsorbate and the work function of the substrate, we refer to it as "potential-driven" hereafter.

For the present study, it is important to note that the LUMO of F4TCNQ molecules lies in the band gap of ZnO. Hence, for intrinsic (undoped) ZnO, one a priori expects no charge-transfer into the LUMO (Figure 1a). In contrast for n-doped ZnO, band bending limited charge transfer occurs into the LUMO of the molecule and the amount of charge transferred should, therefore, depend critically on the charge carrier concentration[30] (Figure 1b shows the energy level diagram for a degenerately doped substrate, where one electrons per molecule is transferred across the interface). In other words, the charge carrier concentration of the substrate can be used as a handle to modify the charge-transfer, rendering this material combination ideal for the present computational study.

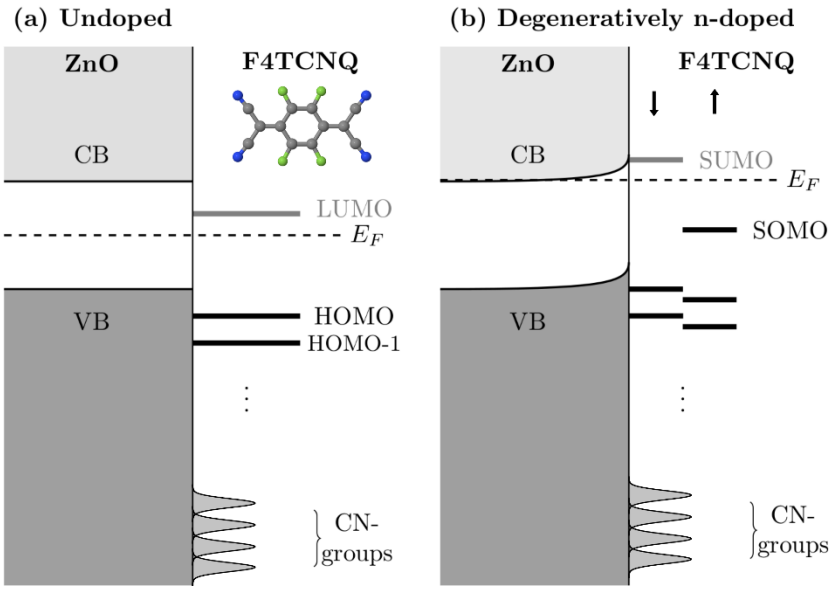

Figure 1. Qualitative level alignment for the F4TCNQ/ZnO interface. (a) shows the level alignment for intrinsic (undoped) ZnO, where only the CN-groups hybridize and no charge transfer into the LUMO is observed (E_F represents the ZnO bulk Fermi level).(b) depicts the qualitative level alignment for degenerately doped ZnO, where charge from bulk dopants is transferred into the LUMO resulting in band bending and a splitting into a SOMO and a SUMO.

The major issue in charge-transfer studies based on density functional theory (DFT) is the choice and impact of the exchange-correlation functional. This is mainly due to the so-called many-electron self-interaction error (MSIE), which leads to the tendency of charge over-delocalization for common local and semilocal functionals.[34–36]. Hybrid functionals, which contain a fraction of Hartree-Fock-like (HF) exchange, in general perform better in in terms of charge transfer, but too much HF exchange leads to the converse problem of over-localizing charge.[35,37,38] Arguably, the best results are obtained when choosing the amount of HF exchange such that the functional becomes MSIE-free. In this case the functional neither over-localizes nor it over-delocalizes charge, and the charge transfer at the interface can be driven into either solution depending on the initialization.[39,40]

For the F4TCNQ molecule, the MSIE-free situation is achieved by using the PBEh[41] functional with 63% HF exchange. Due to screening, the required amount for HF exchange of the F4TCNQ/ZnO interface to achieve MSIE-free behavior would be notably smaller.[39] However, at too low values the

energy level ordering at the interface is no longer correctly reproduced, as the LUMO shifts below the valence band of the ZnO. This gives rise to spurious charge-transfer from the valence band of ZnO.[30] Therefore, the calculations presented in this work were performed with 63% HF exchange, which thus tendentially lead to charge over-localization. We discuss the impact of this at the end of this paper. Further methodological details are given in the method section and the Supporting Information.

The ideal starting point for our investigation is a perfect, intrinsic ZnO substrate. We acknowledge that, to the best of our knowledge, such a substrate is hypothetical, since already trace amounts of hydrogen (e.g., in the residual gas of UHV chambers) lead to n-type doping of ZnO.[42] Nonetheless, because the ionization energy of ZnO (ca. 8 eV) [43] is much larger than the electron affinity of F4TCNQ (EA = 5.2 eV),[44] we do not expect any potential-driven charge (back-)transfer for the intrinsic substrate. Rather, all charge redistributions occurring at the interface should be due to wave-function overlap between substrate and adsorbate, allowing us to first focus on this effect only.

Indeed, as shown in Figure 2b, our DFT calculations yield the F4TCNQ LUMO to be in the ZnO band gap. Although F4TCNQ is a strong electron acceptor, adsorption on intrinsic ZnO leads to a reduction of the work function by -0.83 eV. The reason for this, besides a small molecular dipole induced by the bent geometry on the surface, is that the molecule acquires a small, *positive* Mulliken charge (ca. 0.1 electrons, i.e. the molecules basically remain neutral). In principle, there are several possible reasons for this: Besides covalent interactions, these include Pauli push-back[45] or polarization of the electron cloud. To demonstrate that the positive charge is indeed due to bond formation, in Fig. 2a we plot the line-integrated charge rearrangements upon adsorption of the molecule (i.e, the difference between the charge density of the combined system and the sum of the charge densities of the isolated components, integrated along the line of sight of the figure.). The charge rearrangements are dominated by a reduction of the electron density of C≡N triple bond (red regions) and a concomitant increase between the peripheral nitrogen atoms and the substrate Zn atoms. The overall shape of the charge rearrangements strongly resembles the

cyano-orbitals, that are also relevant for charge donation on variety of other substrates.[16,28] The observation that the adsorption energy of F4TCNQ on ZnO is exothermic (E_{ads} = -2.31 eV) even when disregarding van-der-Waals interactions (which amount to -1.37 eV) further corroborates the notion that this is a covalent interaction due to the hybridization of the substrate's and adsorbate's wave function. Such a chemisorptive bond of the cyano groups with the surface and the associated charge rearrangement is not surprising and is expected also for other adsorbates with functional groups that strongly interact with ionic substrates.

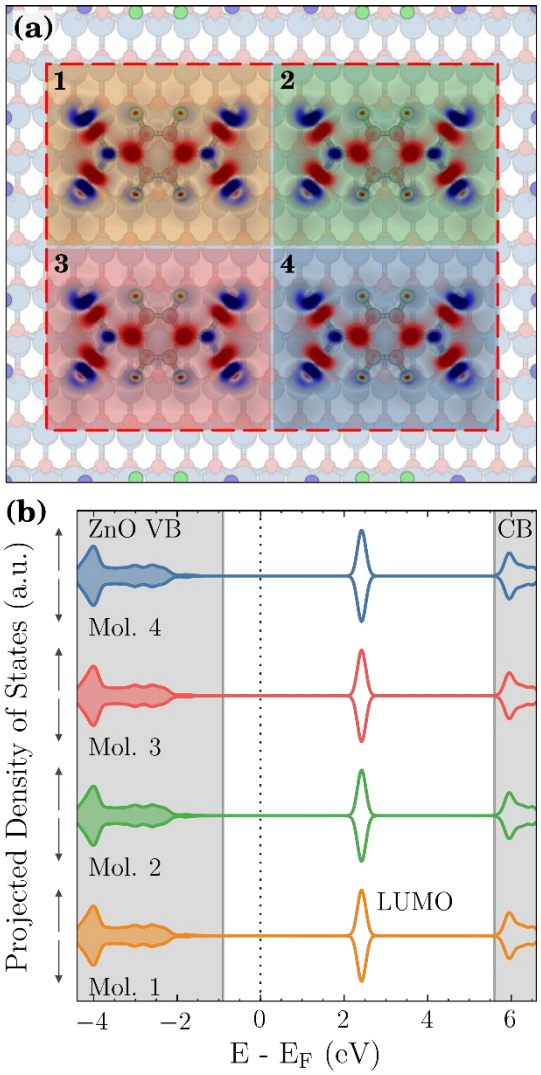

Figure 2. (a) Line-averaged charge rearrangements within the surface supercell containing four F4TCNQ molecules. Blue areas indicate an increase in electron density, red areas a reduced electron

density. (b) DOS projected on the individual molecules adsorbed on undoped ZnO. The gray areas indicate the conduction and valence band of ZnO.

Since in the studied molecular monolayer all molecules are equivalent and the small positive charge transfer originates from local charge rearrangements due to the covalent bonding of the molecules to the surface, the charge remains fully *delocalized* within the closed monolayer. This is shown by calculations of a supercell containing four molecules, i.e. all molecules in the layer remain equivalent as clearly be seen in the charge rearrangement of the four molecules in the supercell as well as in the density of states projected onto the individual molecules (Figure 2).

The situation changes fundamentally for an n-doped substrate. Doping nominally introduces free charge carriers into the conduction band of ZnO. However, as shown in Fig 1a and Fig 2b, for the undoped substrate the (empty) F4TCNQ LUMO lies below the conduction band. Thus, F4TCNQ molecules act as p-dopants at the surface with a very high local concentration. Hence, the energy of the combined system can be lowered if (some of) the introduced charge carriers are transferred to the molecule. However, in contrast to the cyano-groups, the LUMO does not hybridize notably with the substrate. This is evident from Figure 2b by the fact that the orbital remains a sharp peak in the band gap, without additional contributions in resonance in the substrate bands. Hence, any doping-induced charge backdonation from the substrate to the molecule must be a primarily non-covalent, ionic process.

Such charge transfer leads to the formation of an interface dipole between substrate and adsorbate, which shifts the LUMO upwards in energy (relative to the conduction band). This interface dipole is not confined to the region between the components, but, for a doped semiconductor, also extends into the substrate itself – in other words, it leads to band bending, as schematically indicated in Figure 1b. This interface dipole and its associated energetic cost limits how much charge the molecular layer receives. Importantly, this is directly dependent on the charge carrier concentration, and can vary from negligible

charge transfer in the case of low charge carrier concentrations to very large charge transfer for high charge carrier concentrations.[30]

In our simulations, we account for doping using the CREST approach,[46] which allows to explicitly introduce doping in DFT calculations by mimicking the long ranged electrostatic effect of band bending (for further details see SI). Like for the undoped case, we use a supercell (2x2 containing four molecules, see Figure 3a) to conceptually allow for charge localization in the layer. For the following discussion, it is useful to consider the evolution of charge donation (i.e., the contribution of the cyano groups) and backdonation (the filling of the molecular LUMO) separately. We will focus on backdonation first.

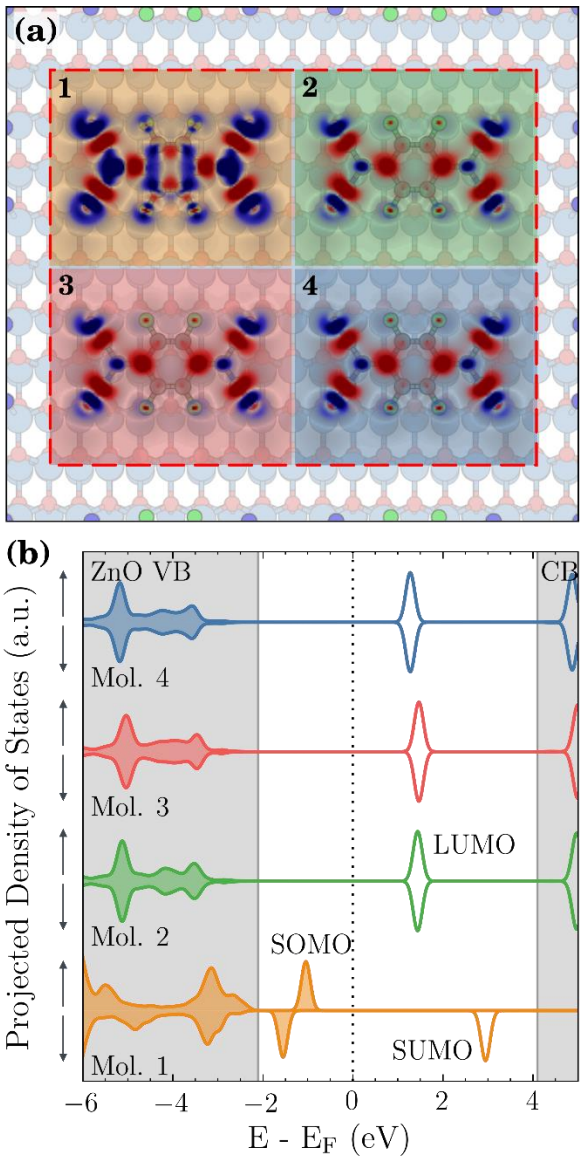

Figure 3. (a) Line-averaged charge rearrangements within the surface supercell containing four F4TCNQ molecules. Blue areas indicate an increase in electron density, red areas a reduced electron density. (b) DOS projected on the individual molecules adsorbed on ZnO with a free carrier concentration of 1.9×10^{19} cm^{-3}. The gray areas indicate the conduction and valence band of ZnO.

Any finite n-type doping activates the backdonation channel. At a charge carrier concentration of 1.9×10^{19} cm^{-3}, ZnO back-donates one electron per supercell, i.e. ¼ electron per F4TCNQ molecule. This exceeds the donated charge, leading to an overlayer that is overall negatively charged, as one would expect for the adsorption of a strong electron acceptor. However, as evident from Figure 3a, our

calculations show that, in contrast to the charge-donation, the backdonated charge is *not* equally distributed. Rather, while all molecules still show the telltale density redistribution of charge donation, only molecule 1 (top left corner) additionally shows charge rearrangements reminiscent of the molecular LUMO. This is further corroborated by the density of states shown in Figure 3b, which shows that the molecule becomes a radical anion, i.e. the LUMO splits into a singly occupied molecular orbital (SOMO) and a single unoccupied molecular orbital (SUMO). Thus, the electron-backtransfer occurs in the same way it would for a free molecule in the gas phase, but is in stark contrast to charge-transfer on metallic surfaces, where no spin-polarization occurs. Interestingly, this means that although the overall charge of the F4TCNQ monolayer is negative on average, at this doping concentration most of the molecules are slightly positively charged.

Furthermore, increasing the carrier concentration increases the charge backdonation: 2, 3, or 4 electrons per supercell are backdonated at charge carrier concentration of approximately 6.4×10^{19}, 1.5×10^{20}, and 2.9×10^{20} cm^{-3}, respectively (see Figure 4). Importantly, the additional charge always localizes onto

individual molecules and renders them radical anionic (i.e. spin-polarized, without molecular density of states at or near the Fermi-edge).

In a previous study[30] similar charge transfer values were found as a function of the free charge carrier concentration using a simpler model, however this study did not consider spin-polarization and focused on the average amount of charge transfer and not its localization.

We can thus conclude that even for degenerate doping, where the charge-carrier concentration is close to that of a metal, the charge-transfer mechanism does not change qualitatively, and the backdonated charge does not become delocalized within the molecular layer as it is on pristine metals.

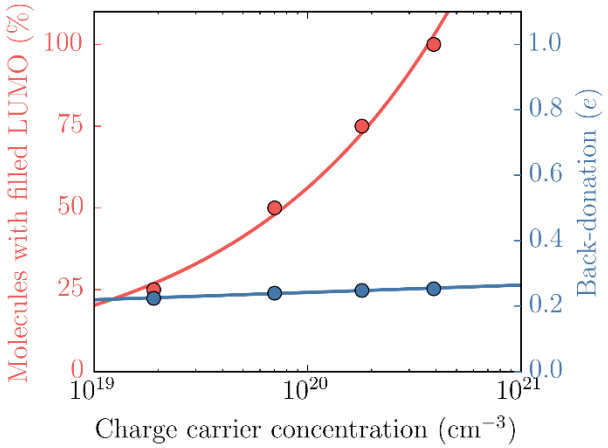

Figure 4. Red: Number of molecules with singly occupied orbitals within the molecular layer as the charge carrier concentration is increased. Blue: Charge donation per molecule from the cyano orbitals only.

In contrast to the backdonation channel, the amount of charge donated by the cyano groups hardly sensitive to the charge carrier concentration in the ZnO. Qualitatively, filling the LUMO of one molecule in the supercell (e.g., at $2x10^{19}$ cm^{-3}), affect neither its own charge-donation significantly, nor that of the other molecules in the unit. This is not surprising, because the bonding character of the cyano groups to the surface does not charge upon charge transfer int the LUMO of the molecule, but it shows that the two

mechanisms, donation and backdonation, are of different nature and act independently of each other. Since the LUMO of some molecules remain unfilled, they still exhibit a small net positive charge, which leads to a coexistence of basically neutral and negatively charged molecules on the surface.

We note at this point that, as mentioned initially, the chosen functional has a tendency to overlocalize charge. This raises the question whether our results might be artefacts from the employed method. However, we stress that we find localization for only one channel and delocalization for the other, rather than localization for both. Moreover, the same qualitative results are obtained when using the default PBE0 functional (which employs a much smaller fraction of HF-like exchange, 25%). Thus, at the very least our results are a proof of concept that different charge localization for different charge-transfer channels, as we have described here, is conceptually possible and can be modelled within hybrid functional DFT. However, since the degree of hybridization (which appears to be the governing factor) is essentially independent of the employed functional, we are also confident that our results are robust and will hold up to experimental scrutiny. Moreover, we expect our findings to be directly transferrable to other semiconductor/organic interfaces which show a combination of charge donation and backdonation. Such systems are, indeed, quite common, and include small molecules frequently used for surface science studies, such as carbon monoxide,[47] as well as large molecules used in the context of organic electronics, such as PTCDA.[48] Furthermore our study show that regarding charge transfer mechanism doped conductive oxides show similar behavior as ultrathin dielectric films on metals. One can conclude that when the LUMO of the molecule does not hybridize with the substrate and is located within the principle bandgap of the semiconductor, integer charge transfer is expected in the case the Fermi level lies above the LUMO energy because of e.g. doping. The situation is similar to systems of ultrathin dielectric films on metals, where the dielectric film prevents the wave function overlap and provides the necessary gap.

In summary, we have investigated the F4TCNQ/ZnO(10-10) interface, which undergoes a charge donation/backdonation reaction. The charge donation is driven by hybridization between the components. It affects all molecules equally, rendering them fractionally positive independent of the doping of the substrate. Conversely, the backdonation is driven by the difference of the component's electron chemical potentials. Our calculations indicate that only some molecules receive an integer electron in the process, rendering them negative. The LUMO of the other molecules at the interface remains empty. This leads to a coexistence of basically neutral and negatively charged molecules on the surface. The number of negatively charged molecules depends critically on the number of free charge-carriers of the substrate (i.e,. its "metallicity"). For low doping concentrations, we find that the number of slightly positive molecules may even exceed that of negative moieties, even if the overall charge of the monolayer is net negative. As we increase the charge carrier concentration the fundamental mechanisms do not change, but the density of molecules within the monolayer with integer charged LUMOs increases. The two mechanisms are found to be essentially independent from each other. This indicates that only the hybridization, and not the "metallicity" of the substrates, determines the charge transfer mechanism, even if the latter plays a major role for the amount of charge transferred.

Methods

All DFT calculations presented here are performed with the FHI-aims package.[49–51] Van der Waals forces are included with the vdW-TS scheme,[52] employing parameters for the substrate that are optimized for ZnO interfaces.[53] The interface is modeled with a four double-layer ZnO surface slab cell that contains four F4TCNQ molecules at a surface area of 548.6 $Å^2$ (See Fig. 2). Geometry relaxations for this surface unit cell were performed using a single Gamma centered k-point (This corresponds to a k-point grid of 8x4x1 for the primitive ZnO (10-10) surface unit cell) and with the default element-specific "light" settings for the integration grids and basis sets. For final single point calculations a reciprocal k-grid of 2x2x1 was used with default "tight" setting (without the "tier-2" f and g basis functions for oxygen). The

k-grid was scaled accordingly for smaller unit cells containing only one molecule. To further reduce memory consumption we increased the Hartree-Fock screening threshold ("crit_val") to 10^{-5}.

The ZnO lattice constant was obtained from a PBE calculation and was kept fixed for all hybrid calculations because geometry optimizations for the ZnO substrate were only performed on the PBE level (see below). We carefully checked that the lattice constant of the substrate has no significant influence on our results. Since in the case of integer charge transfer the system undergoes a symmetry breaking in the charge density that is accompanied by a symmetry breaking in the geometry of the monolayer, it is essential to optimize the geometry of the monolayer for all calculations with the corresponding functional. The geometry relaxation strategy is therefore as follows: The interface was pre-relaxed using the PBE functional, fixing the bottom two double-layers of the substrate at their bulk position while allowing the other layers, as well as the molecules, to relax. The final relaxation was performed with the Perdew-Burke-Ernzerhof hybrid (PBEh) functional with the mixing parameter $\alpha = 0.63$. For all hybrid calculations the substrate was kept fixed and only the molecular monolayer was allowed to relax until the residual forces are smaller than 10^{-4} eV/Å. All electronic structure results reported int his paper were also obtained with this functional. More details about the computations including how we used CREST[46] to mimic the effect of band bending in our DFT calculations and information about the spin-polarized charge density initialization can be found in the supplementary information.

ACKNOWLEDGMENT

The author acknowledges funding from the Austrian Science Fund (FWF: P27868-N36). The computational results presented have been achieved using the Vienna Scientific Cluster (VSC). We thank Egbert Zojer for valuable insights and fruitful discussions.

SUPPORTING INFORMATION

Further computational details (doping and band bending model, spin-polarized charge density initialization), adsorption site and geometry of the monolayer, molecular orbital density of states, discussion on the applied density functional

REFERENCES

(1) Hung, L. S.; Chen, C. H. Recent Progress of Molecular Organic Electroluminescent Materials and Devices. *Mater. Sci. Eng., R* **2002**, *39* (5–6), 143–222. https://doi.org/10.1016/S0927-796X(02)00093-1.

(2) Meredith, P.; Bettinger, C. J.; Irimia-Vladu, M.; Mostert, A. B.; Schwenn, P. E. Electronic and Optoelectronic Materials and Devices Inspired by Nature. *Reports on Progress in Physics* **2013**, *76* (3), 034501. https://doi.org/10.1088/0034-4885/76/3/034501.

(3) Cao, H.; He, W.; Mao, Y.; Lin, X.; Ishikawa, K.; Dickerson, J. H.; Hess, W. P. Recent Progress in Degradation and Stabilization of Organic Solar Cells. *Journal of Power Sources* **2014**, *264*, 168–183. https://doi.org/10.1016/j.jpowsour.2014.04.080.

(4) Kaur, N.; Singh, M.; Pathak, D.; Wagner, T.; Nunzi, J. M. Organic Materials for Photovoltaic Applications: Review and Mechanism. *Synthetic Metals* **2014**, *190*, 20–26. https://doi.org/10.1016/j.synthmet.2014.01.022.

(5) Paulsson, M.; Datta, S. Thermoelectric Effect in Molecular Electronics. *Physical Review B* **2003**, *67* (24). https://doi.org/10.1103/PhysRevB.67.241403.

(6) McNellis, E.; Meyer, J.; Baghi, A.; Reuter, K. Stabilizing a Molecular Switch at Solid Surfaces: A Density Functional Theory Study of Azobenzene on Cu(111), Ag(111), and Au(111). *Physical Review B* **2009**, *80* (3). https://doi.org/10.1103/PhysRevB.80.035414.

(7) Maurer, R. J.; Reuter, K. Bistability Loss as a Key Feature in Azobenzene (Non-)Switching on Metal Surfaces. *Angewandte Chemie* **2012**, *124* (48), 12175–12177. https://doi.org/10.1002/ange.201205718.

(8) Sanvito, S. Molecular Spintronics. *Chemical Society Reviews* **2011**, *40* (6), 3336. https://doi.org/10.1039/c1cs15047b.

(9) Braun, S.; Salaneck, W. R.; Fahlman, M. Energy-Level Alignment at Organic/Metal and Organic/Organic Interfaces. *Advanced Materials* **2009**, *21* (14–15), 1450–1472. https://doi.org/10.1002/adma.200802893.
(10) Braun, S.; Salaneck, W. R. Fermi Level Pinning at Interfaces with Tetrafluorotetracyanoquinodimethane (F4-TCNQ): The Role of Integer Charge Transfer States. *Chem. Phys. Lett.* **2007**, *438* (4–6), 259–262.
(11) Hofmann, O. T.; Rinke, P.; Scheffler, M.; Heimel, G. Integer *versus* Fractional Charge Transfer at Metal(/Insulator)/Organic Interfaces: Cu(/NaCl)/TCNE. *ACS Nano* **2015**, *9* (5), 5391–5404. https://doi.org/10.1021/acsnano.5b01164.
(12) Hofmann, O. T.; Atalla, V.; Moll, N.; Rinke, P.; Scheffler, M. Interface Dipoles of Organic Molecules on Ag(111) in Hybrid Density-Functional Theory. *New Journal of Physics* **2013**, *15* (12), 123028. https://doi.org/10.1088/1367-2630/15/12/123028.
(13) Hollerer, M.; Lüftner, D.; Hurdax, P.; Ules, T.; Soubatch, S.; Tautz, F. S.; Koller, G.; Puschnig, P.; Sterrer, M.; Ramsey, M. G. Charge Transfer and Orbital Level Alignment at Inorganic/Organic Interfaces: The Role of Dielectric Interlayers. *ACS Nano* **2017**, *11* (6), 6252–6260. https://doi.org/10.1021/acsnano.7b02449.
(14) Gruenewald, M.; Schirra, L. K.; Winget, P.; Kozlik, M.; Ndione, P. F.; Sigdel, A. K.; Berry, J. J.; Forker, R.; Bredas, J.-L.; Fritz, T.; et al. Integer Charge Transfer and Hybridization at an Organic Semiconductor / Conductive Oxide Interface. *The Journal of Physical Chemistry C* **2015**, *119* (9), 4865–4873. https://doi.org/10.1021/jp512153b.
(15) Duhm, S.; Glowatzki, H.; Cimpeanu, V.; Klankermayer, J.; Rabe, J. P.; Johnson, R. L.; Koch, N. Weak Charge Transfer between an Acceptor Molecule and Metal Surfaces Enabling Organic/Metal Energy Level Tuning. *J. Phys. Chem. B* **2006**, *110* (42), 21069–21072. https://doi.org/10.1021/jp0644715.
(16) Romaner, L.; Heimel, G.; Brédas, J.-L.; Gerlach, A.; Schreiber, F.; Johnson, R.; Zegenhagen, J.; Duhm, S.; Koch, N.; Zojer, E. Impact of Bidirectional Charge Transfer and Molecular Distortions on the Electronic Structure of a Metal-Organic Interface. *Phys. Rev. Lett.* **2007**, *99* (25), 256801. https://doi.org/10.1103/PhysRevLett.99.256801.
(17) Heimel, G.; Duhm, S.; Salzmann, I.; Gerlach, A.; Strozecka, A.; Niederhausen, J.; Bürker, C.; Hosokai, T.; Fernandez-Torrente, I.; Schulze, G.; et al. Charged and Metallic Molecular Monolayers through Surface-Induced Aromatic Stabilization. *Nature Chemistry* **2013**, *5* (3), 187–194. https://doi.org/10.1038/nchem.1572.
(18) Glowatzki, H.; Bröker, B.; Blum, R.-P.; Hofmann, O. T.; Vollmer, A.; Rieger, R.; Müllen, K.; Zojer, E.; Rabe, J. P.; Koch, N. "Soft" Metallic Contact to Isolated C 60. *Nano Lett.* **2008**, *8* (11), 3825–3829. https://doi.org/10.1021/nl8021797.
(19) Crispin, X.; Geskin, V.; Crispin, A.; Cornil, J.; Lazzaroni, R.; Salaneck, W. R.; Brédas, J.-L. Characterization of the Interface Dipole at Organic/ Metal Interfaces. *J. Am. Chem. Soc.* **2002**, *124* (27), 8131–8141. https://doi.org/10.1021/ja025673r.
(20) Roth, A. P.; Webb, J. B.; Williams, D. F. Absorption Edge Shift in ZnO Thin Films at High Carrier Densities. *Solid State Communications* **1981**, *39* (12), 1269–1271. https://doi.org/10.1016/0038-1098(81)90224-6.
(21) Srikant, V.; Clarke, D. R. On the Optical Band Gap of Zinc Oxide. *Journal of Applied Physics* **1998**, *83* (10), 5447–5451. https://doi.org/10.1063/1.367375.
(22) Look, D. C.; Reynolds, D. C.; Sizelove, J. R.; Jones, R. L.; Litton, C. W.; Cantwell, G.; Harsch, W. C. Electrical Properties of Bulk ZnO. *Solid State Communications* **1998**, *105* (6), 399–401. https://doi.org/10.1016/S0038-1098(97)10145-4.

(23) Hu, J.; Gordon, R. G. Textured Aluminum-doped Zinc Oxide Thin Films from Atmospheric Pressure Chemical-vapor Deposition. *Journal of Applied Physics* **1992**, *71* (2), 880–890. https://doi.org/10.1063/1.351309.
(24) Ko, H. J.; Chen, Y. F.; Hong, S. K.; Wenisch, H.; Yao, T.; Look, D. C. Ga-Doped ZnO Films Grown on GaN Templates by Plasma-Assisted Molecular-Beam Epitaxy. *Applied Physics Letters* **2000**, *77* (23), 3761–3763. https://doi.org/10.1063/1.1331089.
(25) Kalusniak, S.; Sadofev, S.; Schäfer, P.; Henneberger, F. Heavily N-Type ZnO: A Plasmonic Material at Telecommunication Wavelengths: Heavily n-Type ZnO: A Plasmonic Material at Telecommunication Wavelengths. *physica status solidi (c)* **2014**, *11* (7–8), 1357–1360. https://doi.org/10.1002/pssc.201300738.
(26) Chen, D.-Y.; Tseng, W.-H.; Liang, S.-P.; Wu, C.-I.; Hsu, C.-W.; Chi, Y.; Hung, W.-Y.; Chou, P.-T. Application of F4TCNQ Doped Spiro-MeOTAD in High Performance Solid State Dye Sensitized Solar Cells. *Physical Chemistry Chemical Physics* **2012**, *14* (33), 11689. https://doi.org/10.1039/c2cp41855j.
(27) Liu, D.; Li, Y.; Yuan, J.; Hong, Q.; Shi, G.; Yuan, D.; Wei, J.; Huang, C.; Tang, J.; Fung, M.-K. Improved Performance of Inverted Planar Perovskite Solar Cells with F4-TCNQ Doped PEDOT:PSS Hole Transport Layers. *Journal of Materials Chemistry A* **2017**, *5* (12), 5701–5708. https://doi.org/10.1039/C6TA10212C.
(28) Rangger, G.; Hofmann, O.; Romaner, L.; Heimel, G.; Bröker, B.; Blum, R.-P.; Johnson, R.; Koch, N.; Zojer, E. F4TCNQ on Cu, Ag, and Au as Prototypical Example for a Strong Organic Acceptor on Coinage Metals. *Phys. Rev. B* **2009**, *79* (16). https://doi.org/10.1103/PhysRevB.79.165306.
(29) Gerbert, D.; Hofmann, O. T.; Tegeder, P. Formation of Occupied and Unoccupied Hybrid Bands at Interfaces between Metals and Organic Donors/Acceptors. *The Journal of Physical Chemistry C* **2018**, *122* (48), 27554–27560. https://doi.org/10.1021/acs.jpcc.8b09606.
(30) Xu, Y.; Hofmann, O. T.; Schlesinger, R.; Winkler, S.; Frisch, J.; Niederhausen, J.; Vollmer, A.; Blumstengel, S.; Henneberger, F.; Koch, N.; et al. Space-Charge Transfer in Hybrid Inorganic-Organic Systems. *Physical Review Letters* **2013**, *111* (22), 226802. https://doi.org/10.1103/PhysRevLett.111.226802.
(31) Mukai, K.; Yoshinobu, J. Observation of Charge Transfer States of F4-TCNQ on the 2-Methylpropene Chemisorbed Si(100)(2×1) Surface. *Journal of Electron Spectroscopy and Related Phenomena* **2009**, *174* (1–3), 55–58. https://doi.org/10.1016/j.elspec.2009.04.006.
(32) Topham, B. J.; Kumar, M.; Soos, Z. G. Profiles of Work Function Shifts and Collective Charge Transfer in Submonolayer Metal-Organic Films. *Advanced Functional Materials* **2011**, *21* (10), 1931–1940. https://doi.org/10.1002/adfm.201002677.
(33) Koch, N. Organic Electronic Devices and Their Functional Interfaces. *ChemPhysChem* **2007**, *8* (10), 1438–1455. https://doi.org/10.1002/cphc.200700177.
(34) Mori-Sánchez, P.; Cohen, A. J.; Yang, W. Many-Electron Self-Interaction Error in Approximate Density Functionals. *J. Chem. Phys.* **2006**, *125* (20), 201102. https://doi.org/10.1063/1.2403848.
(35) Cohen, A. J.; Mori-Sanchez, P.; Yang, W. Insights into Current Limitations of Density Functional Theory. *Science* **2008**, *321* (5890), 792–794. https://doi.org/10.1126/science.1158722.
(36) Zheng, X.; Liu, M.; Johnson, E. R.; Contreras-García, J.; Yang, W. Delocalization Error of Density-Functional Approximations: A Distinct Manifestation in Hydrogen Molecular Chains. *The Journal of Chemical Physics* **2012**, *137* (21), 214106. https://doi.org/10.1063/1.4768673.
(37) Gani, T. Z. H.; Kulik, H. J. Where Does the Density Localize? Convergent Behavior for Global Hybrids, Range Separation, and DFT+U. *Journal of Chemical Theory and Computation* **2016**, *12* (12), 5931–5945. https://doi.org/10.1021/acs.jctc.6b00937.

(38) Atalla, V.; Zhang, I. Y.; Hofmann, O. T.; Ren, X.; Rinke, P.; Scheffler, M. Enforcing the Linear Behavior of the Total Energy with Hybrid Functionals: Implications for Charge Transfer, Interaction Energies, and the Random-Phase Approximation. *Physical Review B* **2016**, *94* (3), 035140. https://doi.org/10.1103/PhysRevB.94.035140.
(39) Wruss, E.; Zojer, E.; Hofmann, O. T. Distinguishing between Charge-Transfer Mechanisms at Organic/Inorganic Interfaces Employing Hybrid Functionals. *The Journal of Physical Chemistry C* **2018**, *122* (26), 14640–14653. https://doi.org/10.1021/acs.jpcc.8b03699.
(40) Sai, N.; Barbara, P. F.; Leung, K. Hole Localization in Molecular Crystals from Hybrid Density Functional Theory. *Physical Review Letters* **2011**, *106* (22), 226403. https://doi.org/10.1103/PhysRevLett.106.226403.
(41) Perdew, J. P.; Ernzerhof, M.; Burke, K. Rationale for Mixing Exact Exchange with Density Functional Approximations. *The Journal of Chemical Physics* **1996**, *105* (22), 9982. https://doi.org/10.1063/1.472933.
(42) Van de Walle, C. G. Hydrogen as a Cause of Doping in Zinc Oxide. *Physical Review Letters* **2000**, *85* (5), 1012–1015. https://doi.org/10.1103/PhysRevLett.85.1012.
(43) Woll, C. The Chemistry and Physics of Zinc Oxide Surfaces. *Progress in Surface Science* **2007**, *82* (2–3), 55–120. https://doi.org/10.1016/j.progsurf.2006.12.002.
(44) Gao, W.; Kahn, A. Controlled *p* -Doping of Zinc Phthalocyanine by Coevaporation with Tetrafluorotetracyanoquinodimethane: A Direct and Inverse Photoemission Study. *Applied Physics Letters* **2001**, *79* (24), 4040–4042. https://doi.org/10.1063/1.1424067.
(45) Bagus, P.; Käfer, D.; Witte, G.; Wöll, C. Work Function Changes Induced by Charged Adsorbates: Origin of the Polarity Asymmetry. *Physical Review Letters* **2008**, *100* (12). https://doi.org/10.1103/PhysRevLett.100.126101.
(46) Erker, S.; Rinke, P.; Moll, N.; Hofmann, O. T. Doping Dependence of the Surface Phase Stability of Polar O-Terminated (000$\bar{1}$) ZnO. *New Journal of Physics* **2017**, *19* (8), 083012. https://doi.org/10.1088/1367-2630/aa79e7.
(47) Blyholder, G. Molecular Orbital View of Chemisorbed Carbon Monoxide. *The Journal of Physical Chemistry* **1964**, *68* (10), 2772–2777.
(48) Tautz, F. S. Structure and Bonding of Large Aromatic Molecules on Noble Metal Surfaces: The Example of PTCDA. *Progress in Surface Science* **2007**, *82* (9–12), 479–520. https://doi.org/10.1016/j.progsurf.2007.09.001.
(49) Blum, V.; Gehrke, R.; Hanke, F.; Havu, P.; Havu, V.; Ren, X.; Reuter, K.; Scheffler, M. Ab Initio Molecular Simulations with Numeric Atom-Centered Orbitals. *Computer Physics Communications* **2009**, *180* (11), 2175–2196. https://doi.org/10.1016/j.cpc.2009.06.022.
(50) Ren, X.; Rinke, P.; Blum, V.; Wieferink, J.; Tkatchenko, A.; Sanfilippo, A.; Reuter, K.; Scheffler, M. Resolution-of-Identity Approach to Hartree–Fock, Hybrid Density Functionals, RPA, MP2 and *GW* with Numeric Atom-Centered Orbital Basis Functions. *New Journal of Physics* **2012**, *14* (5), 053020. https://doi.org/10.1088/1367-2630/14/5/053020.
(51) Ihrig, A. C.; Wieferink, J.; Zhang, I. Y.; Ropo, M.; Ren, X.; Rinke, P.; Scheffler, M.; Blum, V. Accurate Localized Resolution of Identity Approach for Linear-Scaling Hybrid Density Functionals and for Many-Body Perturbation Theory. *New Journal of Physics* **2015**, *17* (9), 093020. https://doi.org/10.1088/1367-2630/17/9/093020.
(52) Tkatchenko, A.; Scheffler, M. Accurate Molecular Van Der Waals Interactions from Ground-State Electron Density and Free-Atom Reference Data. *Physical Review Letters* **2009**, *102* (7), 073005. https://doi.org/10.1103/PhysRevLett.102.073005.
(53) Hofmann, O. T.; Deinert, J.-C.; Xu, Y.; Rinke, P.; Stähler, J.; Wolf, M.; Scheffler, M. Large Work Function Reduction by Adsorption of a Molecule with a Negative Electron Affinity: Pyridine on

ZnO(10-10). *The Journal of Chemical Physics* **2013**, *139* (17), 174701. https://doi.org/10.1063/1.4827017.